Glycogen Synthase Kinase-3 Mediates Acetaminophen-Induced Apoptosis in Human Hepatoma Cells

Patricia Macanas-Pirard, Nik-Soriani Yaacob,[1] Pauline C. Lee,[2] Julie C. Holder, Richard H. Hinton, and George E. N. Kass

School of Biomedical and Molecular Sciences, University of Surrey, Guildford, Surrey, United Kingdom (P.M.-P., N.-S.Y., R.H.H., G.E.N.K.); and Cellular Pathology and Toxicology, GlaxoSmithKline, Ware, United Kingdom (P.C.L., J.C.H.)

ABSTRACT

The mild analgesic drug acetaminophen (AAP) induces severe hepatic injury when taken at excessive doses. Recent evidence shows that the initial form of damage is through apoptosis, but this fails to go to completion and degenerates into necrosis. The aim of this study was to elucidate the mechanism through which AAP induces apoptosis using human HuH7 hepatoma cells as an in vitro model system to investigate the initial phase of AAP-induced hepatic injury. AAP-induced apoptosis in HuH7 cells as evidenced by chromatin condensation was preceded by the translocation of Bax to mitochondria and the cytoplasmic release of the proapoptotic factors cytochrome c and Smac/DIABLO. A concomitant loss of mitochondrial membrane potential occurred. Activation of the mitochondrial pathway of apoptosis led to the activation of execution caspases-3 and -7. AAP-induced apoptosis and cell death was blocked by inhibitors of caspases but not by inhibitors of calpains, cathepsins, and serine proteases. Apoptosis was unaffected by inhibitors of the mitochondrial permeability transition pore and by inhibitors of Jun NH_2-terminal kinases, p38 mitogen-activated protein kinase, or mitogen-activated protein kinase kinase 1/2. However, pharmacological inhibition of glycogen synthase kinase-3 (GSK-3) delayed and decreased the extent of AAP-induced apoptosis. In comparison, endoplasmic reticulum stress-induced but not prooxidant-induced apoptosis of HuH7 cells was sensitive to GSK-3 inhibition. It is concluded that AAP-induced apoptosis involves the mitochondrial pathway of apoptosis that is mediated by GSK-3 and most likely initiated through an endoplasmic reticulum stress response.

The mild analgesic acetaminophen (paracetamol, AAP) remains the commonest cause of acute liver failure in the United States and other parts of the world as a result of accidental or deliberate overdose (Dargan and Jones, 2003). At therapeutic doses, AAP is primarily eliminated as its glucuronide and sulfate conjugate, although a minor portion becomes bioactivated in the liver by CYP2E1 (Tonge et al.,

1998; Zaher et al., 1998) to the reactive metabolite N-acetyl-p-benzoquinoneimine (NAPQI). However, after an AAP overdose the rate and quantity of NAPQI production exceeds its detoxification through conjugation with glutathione, and hepatotoxicity ensues as a consequence of the binding of NAPQI to cellular proteins (Cohen et al., 1997; Qiu et al., 1998) and their oxidative damage (Tirmenstein and Nelson, 1990). A contribution to AAP hepatotoxicity also comes from the release of soluble proinflammatory and proapoptotic molecules such as tumor necrosis factor (Blazka et al., 1996).

Many of the histochemical and biochemical features of the late stages of AAP toxicity, particularly after high doses, support the conclusion that AAP induces hepatocellular necrosis (Adams et al., 2001; Gujral et al., 2002; Knight and Jaeschke, 2002; Pierce et al., 2002; Jaeschke et al., 2004).

ABBREVIATIONS: AAP, acetaminophen; NAPQI, N-acetyl-p-benzoquinoneimine; GSK-3, glycogen synthase kinase-3; ER, endoplasmic reticulum; SB-216763, 3-(2,4-dichlorophenyl)-4-(1-methyl-1H-indol-3-yl)-1H-pyrrole-2,5-dione; SB-415286, 3-[(3-chloro-4-hydroxy phenyl)amino]-4-(2-nitrophenyl)-1H-pyrrol-2,5-dione; PD 150606, 3-(4-iodiophenyl)-2-mercapto-(Z)-2-propenoic acid; PD 98059, 2′-amino-3′-methoxyflavone; SB-203580, 4-(4-fluorophenyl)-2-(4-methylsulfinylphenyl)-5-(4-pyridyl) 1H-imidazole; Z-VAD-fmk, benzyloxycarbonyl-Val-Ala-DL-Asp-fluoromethylketone; Ac-DEVD-CHO, N-acetyl-Asp-Glu-Val-Asp-aldehyde; Z-FA-fmk, Z-Phe-Ala-fmk; MG-132, Z-Leu-Leu-Leu-CHO; TMRE, tetramethylrhodamine ethyl ester; Hsc, heat shock cognate protein; SAPK, stress-activated protein kinase; JNK, c-Jun NH_2-terminal kinase; PBS, phosphate-buffered saline; GSH, glutathione; Smac/DIABLO, second mitochondria-derived activator of caspase/direct inhibitor of apoptosis-binding protein with low pI; $\Delta\Psi m$, mitochondrial membrane potential; PTP, permeability transition pore; MAP, mitogen-activated protein; SP 600125, 1,9-pyrazoloanthrone.

However, several reports have presented evidence for the occurrence of apoptosis in AAP-induced hepatic damage. For instance, AAP toxicity in rats is accompanied by an increase, albeit small, in the number of isolated parenchymal cells with apoptotic morphology (Dixon et al., 1975; Gujral et al., 2002), the formation of oligonucleosomal-length DNA fragmentation (Ray et al., 1990) and the appearance of terminal deoxynucleotidyl transferase-catalyzed dUTP-fluorescein nick end labeling-positive nuclei that were highly condensed (El-Hassan et al., 2003). Several early mitochondrial events linked to apoptosis have been documented, including the truncation of the BH3-only proapoptotic Bcl-2 family member Bid and its relocation to mitochondria (El-Hassan et al., 2003), Bax translocation to mitochondria (Adams et al., 2001; El-Hassan et al., 2003), and the release of mitochondrial cytochrome *c* (Adams et al., 2001; Ferret et al., 2001; Knight and Jaeschke, 2002; El-Hassan et al., 2003). However, there is little or no activation of the execution caspases-3 or -7 in liver tissues (Ferret et al., 2001; Knight and Jaeschke, 2002; Pierce et al., 2002; El-Hassan et al., 2003), and it can be concluded that AAP induces a hepatocellular apoptotic response that fails to go to completion and instead degenerates into necrosis (Adams et al., 2001; Pierce et al., 2002; El-Hassan et al., 2003; Jaeschke et al., 2004). However, the critical role of apoptosis in eliciting AAP-induced liver injury was demonstrated by a report from our laboratory showing that inhibitors of caspases protect mice from AAP-induced hepatic injury and ultimately necrosis in vivo by blocking the activation of the mitochondrial pathway of apoptosis (El-Hassan et al., 2003).

The cytotoxicity of AAP in cultured hepatocytes requires concentrations of the drug that are higher than those required to induce hepatotoxicity in vivo (Prescott, 1996) and is much slower to develop than in mice. More importantly, cultured hepatocytes exposed to AAP die by necrosis in a mechanism that, unlike the situation in vivo (El-Hassan et al., 2003), does not involve cytochrome *c* release from mitochondria and that does not involve or depend on caspases (Neuman et al., 1999; Nagai et al., 2002). In this study, HuH7 hepatoma cells were used as an in vitro model to specifically study the early events that lead to the induction of apoptosis by the hepatotoxic drug. We report here that AAP activated the mitochondrial pathway of apoptosis in a mechanism that was mediated by the release of proapoptotic mitochondrial proteins. The apoptotic response required glycogen synthase kinase-3 (GSK-3) activity through a mechanism that seemed to involve an endoplasmic reticular (ER) stress response.

Materials and Methods

Reagents and Antibodies. Acetaminophen (99% pure), digitonin, *N*-tosyl-L-phenylalanine chloromethyl ketone, saponin, SB-216763, SB-415286, and propidium iodide were purchased from Sigma Chemical (Poole, Dorset, UK). Duroquinone was purchased from Aldrich Chemical Co. (Milwaukee, WI). Benzyloxycarbonyl-Val-Ala-DL-Asp-fluoromethylketone (Z-VAD-fmk) and *N*-acetyl-Asp-Glu-Val-Asp-aldehyde (Ac-DEVD-CHO) were obtained from Bachem (Bubendorf, Switzerland). Z-Phe-Ala-fmk (Z-FA-fmk) was obtained from Enzyme Systems Products (Livermore, CA). Z-Leu-Leu-Leu-CHO (MG-132), thapsigargin, *N*-acetyl-Leu-Leu-Nle-CHO, PD 150606, PD 98059, SB-203580, bongkrekic acid, cyclosporin A, and 1,9-pyrazoloanthrone (SP600125) were purchased from Calbiochem-Novabiochem (Nottingham, UK), and staurosporine and puromycin

were from Alexis Corporation (Nottingham, UK). Bisbenzimide (Hoechst 33258) and tetramethylrhodamine ethyl ester (TMRE) were from Molecular Probes (Eugene, OR). Pefabloc, phenylmethylsulfonyl fluoride, aprotinin, pepstatin, leupeptin, and lactate dehydrogenase cytotoxicity detection kit were purchased from Roche Diagnostics (Indianapolis, IN). Anti-cytochrome *c* antibodies (clones 7H8.2C12 and 6H2.B4 for Western blot analysis and immunocytochemistry, respectively) and phycoerythrin-conjugated anti-caspase-3 (active form) (clone C92–605) were purchased from BD Biosciences PharMingen (San Diego, CA). Anti-cytochrome *c* oxidase (subunit IV) was obtained from Molecular Probes (clone 20E8-C12). Anti-α-fodrin and anti-cytokeratin-18 (cleaved, M30) were obtained from Affiniti Research Products (Golden, CO) and Roche Diagnostics, respectively. Antisera against caspase-3 and Bax (B-9) were obtained from Calbiochem-Novabiochem and Santa Cruz Biotechnology, Inc. (Santa Cruz, CA), respectively. Anti-phospho-SAPK/JNK (Thr183/Tyr185) antibodies, anti-Hsc70 antibodies, and anti-SAPK1b/JNK3 rabbit antibodies were purchased from Cell Signaling Technology Inc. (Beverly, MA), StressGen Biotechnologies (San Diego, CA), and Upstate Biotechnology (Lake Placid, NY), respectively. Anti-caspase-7 and anti-Smac/DIABLO antibodies were a gift from Prof. Gerald M. Cohen (MRC Toxicology Unit, Leicester, UK). All secondary horseradish peroxidase-conjugated and fluorescein isothiocyanate-conjugated antibodies were from DakoCytomation Ltd. (Ely, Cambridgeshire, UK). All other reagents were of analytical grade.

Cell Culture and Treatments. Human hepatoma HuH7 cells (a gift from Prof. R. Bartenschlager, University of Mainz, Mainz, Germany) were grown at 37°C in Dulbecco's modified Eagle's medium supplemented with 10% fetal bovine serum, 100 IU/ml penicillin, and 100 μg/ml streptomycin, nonessential amino acids, and 2 mM L-glutamine in an humidified incubator with 5% carbon dioxide, 95% air. The cells were exposed in medium supplemented with 2% fetal bovine serum to AAP in the absence or presence of modulators of apoptosis (or a corresponding volume of solvent) as described under *Results*. The final concentration of solvent never exceeded 0.1% (v/v).

Analysis of Apoptosis and Cell Death. Changes in nuclear morphology were assessed by fixing the cells grown on poly-L-lysine-coated glass coverslips in 4% (v/v) formaldehyde at room temperature for 30 min. The fixed cells were stained with 2 μg/ml Hoechst 33258, and nuclear morphology was analyzed by fluorescence microscopy. The nuclei were scored as either normal, in which the chromatin was uncondensed, or apoptotic, in which the chromatin was highly condensed or fragmented into discrete apoptotic bodies (Jones et al., 1998). The assessment of cell viability was performed using the lactate dehydrogenase cytotoxicity detection kit according to the manufacturer's instructions. DNA fragmentation was analyzed by flow cytometric detection of hypodiploid DNA. In brief, cells were detached by trypsinization, combined with medium containing floating cells, and centrifuged at 100*g* for 5 min. The pellets were fixed in ice-cold 70% (v/v) ethanol in PBS overnight at 4°C by gradual addition while vortex mixing. The cells were subsequently stained with 10 μg/ml propidium iodide and treated with 1 mg/ml RNase for 30 min at 37°C before analysis using a Beckman Coulter Epics XL flow cytometer (argon laser, excitation wavelength 488 nm). A minimum of 20,000 events were acquired in list mode while gating the forward and side scatters to exclude propidium iodide-positive cell debris and analyzed in FL-3 for the appearance of the sub-G_1 peak. Cellular GSH was measured using the Oxis Research Bioxytech GSH-400 kit on a clinical analyzer (SpACE), and ATP content was assayed by luciferin/luciferase.

Analysis of Procaspase Processing and Caspase Substrate Cleavage. Western blot analysis was performed as reported previously (Jones et al., 1998). Cell extracts were prepared in cell lysis buffer [50 mM Tris and 150 mM NaCl, pH 7.5, supplemented with 1% (v/v) Nonidet P-40, 0.2% (w/v) SDS, 1 mM Pefabloc, 2 μg/ml aprotinin, 2 μg/ml leupeptin, 1 mM phenylmethylsulfonyl fluoride, and 1 mM Na_3VO_4]. To separate mitochondrial proteins from cytosolic proteins, the cells were washed, resuspended in intracellular medium buffer (20 mM NaCl, 100 mM KCl, 2 mM $MgCl_2$, 1 mM

EGTA, and 23 mM HEPES, pH 7.1) supplemented with 1 μM cyclosporin A and permeabilized on ice for 10 min by the addition of 1 mg/ml saponin. The cells were then centrifuged (2000g for 5 min at 4°C) to separate cytosolic proteins from membrane (mitochondria)-associated proteins. Protein concentration in the cell samples was assessed using the Bio-Rad protein assay (Bio-Rad, Hercules, CA). The cellular proteins were resolved by SDS-polyacrylamide gel electrophoresis using 7.5 or 15% gels, blotted onto Hybond-C nitrocellulose membranes, and probed with antibodies raised against caspase-3 (1:1000), caspase-7 (1:2000), Bax (1:500), cytochrome c (1:500), cytochrome c oxidase (1:1000), fodrin (1:2000), Smac/DIABLO (1:1000), Hsc70 (1:1000), phospho-SAPK/JNK (1:1000), or SAPK1b/JNK3 (1:1000). Incubation with primary antibodies was carried out overnight at 4°C in an orbital roller. After washing and incubation with peroxidase-conjugated secondary antibody (1:1000), the blots were visualized using the SuperSignal West Pico chemiluminescent detection system (Pierce Chemical, Rockford, IL). The reprobing for loading controls was carried out as described previously (Kaufmann, 2001). In brief, the Hybond-C nitrocellulose membranes were incubated in 15 ml of PBS supplemented with 1 mM sodium azide for 2 h. The membranes were then rinsed in 1× Tris-buffered saline-Tween buffer for 5 min and reprobed with primary antibody. Caspase-3 processing and caspase-mediated cytokeratin-18 cleavage were measured by flow cytometric detection of the corresponding neoepitopes as described by the manufacturers (BD Biosciences PharMingen and Roche Diagnostics, respectively). A minimum of 10,000 events were acquired in list mode while gating the forward and side scatters to exclude cell debris and analyzed in FL-2 and FL-1, respectively, for the appearance of the neoepitopes.

Immunolocalization of Cytochrome c. HuH7 cells grown on poly-L-lysine-coated glass coverslips were fixed with 4% paraformaldehyde buffer for 30 min at room temperature. After washes with blocking buffer (PBS supplemented with 3% bovine serum albumin and 0.05% saponin), the cells were incubated with anti-cytochrome c antibody (1:100 in blocking buffer) overnight at 4°C followed by fluorescence-activated cell sorting-linked secondary antibody (1:100) for 1 h at room temperature and stained with 2 μg/ml Hoechst 33258.

Detection of Mitochondrial Membrane Potential with TMRE. HuH7 cells grown on poly-L-lysine-coated round glass coverslips were treated with AAP, washed with prewarmed PBS, and incubated at 37°C for 15 min with medium supplemented with 2% fetal bovine serum, 0.5 μM TMRE, and 2 μg/ml Hoechst 33258. The cells were then immediately viewed under a Zeiss Axiovert 135 fluorescence microscope.

Statistical Analysis. All data are given as means ± S.D. of at least three independent experiments. Comparison of treatments against controls was made using one-way Analysis of variance followed by Fisher's least significant difference post hoc test with the SPSS statistical package (SPSS Inc., Chicago, IL). The significance level chosen for the statistical analysis was $p < 0.05$.

Results

AAP Induces Apoptosis in HuH7 Cells. A human hepatoma cell line, HuH7, was used to investigate the mechanism of AAP-induced apoptosis induction in vitro. AAP induced a concentration- and time-dependent loss in cell viability in HuH7 cells. The losses of viability at 24 h [as measured by the 3-(4,5-dimethylthiazol-2-yl)-2,5-diphenyltetrazolium assay] after AAP dosing were 21% (1 mM AAP), 24% (5 mM AAP), and 28% (10 mM AAP) and at 48 h were 19% (1 mM AAP), 46% (5 mM AAP), and 68% (10 mM AAP). The loss of cell viability after exposure to 10 mM AAP (Fig. 1) was characterized by the appearance of a large number of cells displaying nuclear apoptotic morphology (chromatin condensation and fragmentation) and DNA fragmen-
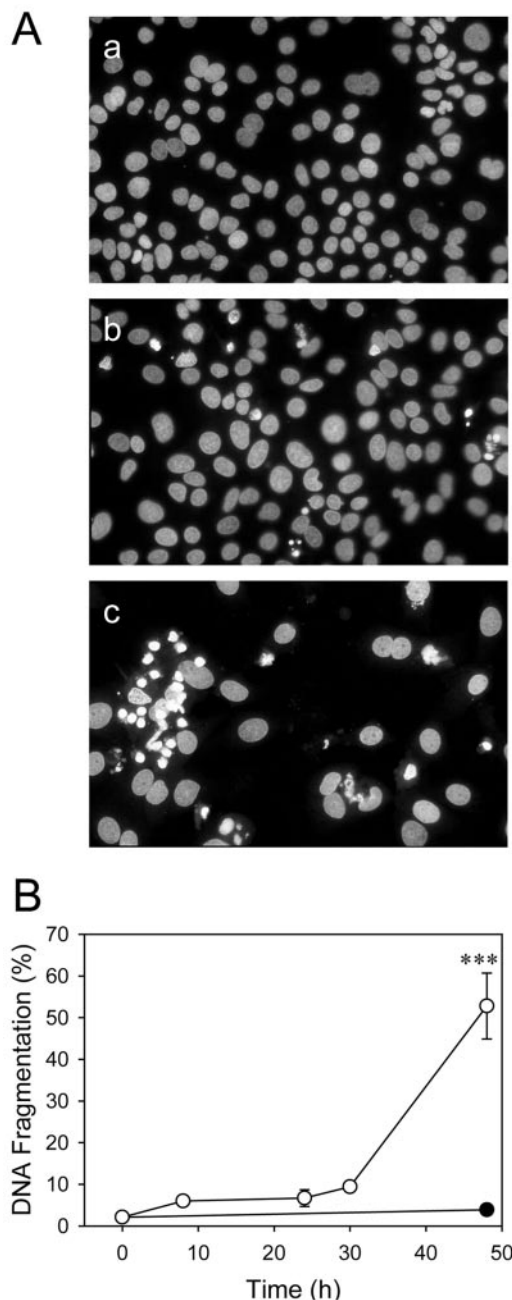
Fig. 1. Acetaminophen induces apoptosis in HuH7 cells. A, HuH7 cells were treated in the absence (a) or presence of AAP (10 mM) for 24 h (b) or 48 h (c) before fixing, staining with Hoechst 33258, and visualization by fluorescence microscopy. B, HuH7 cells were treated in the absence (closed circles) or presence of 10 mM AAP (open circles), and at the indicated time points the cells were harvested, stained with propidium iodide, and analyzed for their DNA content by flow cytometry as described under *Materials and Methods*. Each point is the mean ± S.D. of three independent experiments. ***, $p < 0.001$.

tation. Chromatin condensation also occurred after exposure to 5 mM AAP, although in a reduced number of cells, and only a few isolated apoptotic cells were observed after a 48-h treatment with 1 mM AAP (data not shown). The time course of the development of the cytotoxicity in HuH7 cells followed that occurring in humans where typically 24 to 48 h is required before transaminases, bilirubin levels, and prothrombin time begin to increase (Salgia and Kosnik, 1999). The analysis of biochemical events preceding the loss of HuH7

cell viability and apoptosis showed a decrease in cellular GSH content (53 ± 12 and $39 \pm 4\%$ decrease at 30 and 48 h, respectively) and ATP content (65 ± 5 and $35 \pm 1\%$ decrease at 30 and 48 h, respectively) in response to 10 mM AAP exposure. These findings support a mechanism whereby AAP requires bioactivation to NAPQI for toxicity and apoptosis to occur and that the apoptotic response is concentration-dependent.

Activation and Role of Caspases in AAP-Induced Apoptosis. Extracts from cells treated with AAP were analyzed by Western blotting for the processing and activation of the execution caspases-3 and -7. Solvent control-treated cells showed the distinct presence of procaspase-3 (p32) and a second band possibly corresponding to caspase-3 minus the prodomain (p29) (Fig. 2A). Treatment of HuH7 cells with the apoptosis-inducing drugs staurosporine (1 μM for 24 h) or puromycin (20 μM for 24 h) generated a band that corresponded to the active fragment p17. This band was absent from control cells but was detected in HuH7 cells treated with 10 mM AAP for 24 or 48 h (Fig. 2A). This supports the conclusion that AAP-induced apoptosis correlated with the proteolytic processing and activation of caspase-3 in HuH7 cells. A fourth immunoreactive (p20) band was present in all samples. The latter band could have corresponded to the large subunit plus prodomain that in a cellular environment as p20-p12 complex is inactive (Li et al., 2002). To address this possibility, we investigated the processing of caspase-3 by flow cytometry using an antibody specifically recognizing the p20/p17 large fragments of caspase-3 but not the inactive proform. The lack of immunoreactivity in control cells demonstrates that the 20-kDa band detected by Western blot was unrelated to the p20 large subunit of caspase-3. Most importantly, Fig. 2B shows that the time course of the appearance of the active caspase-3 correlated with the induction of apoptosis. Similarly, immunoblotting for caspase-7 revealed that this executioner caspase was similarly activated by AAP as evidenced by the appearance of the large fragment, p19 (Fig. 2A).
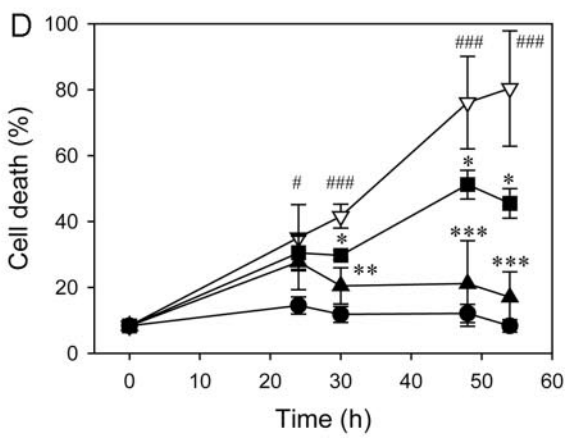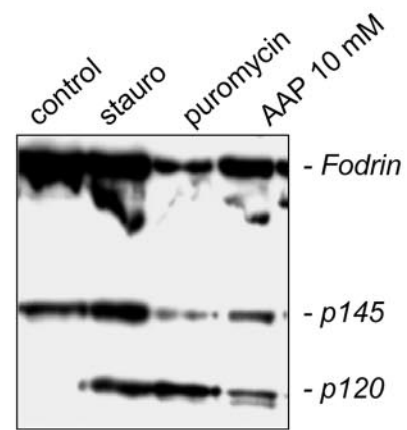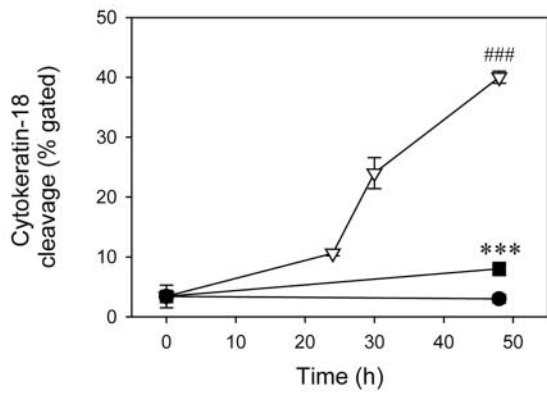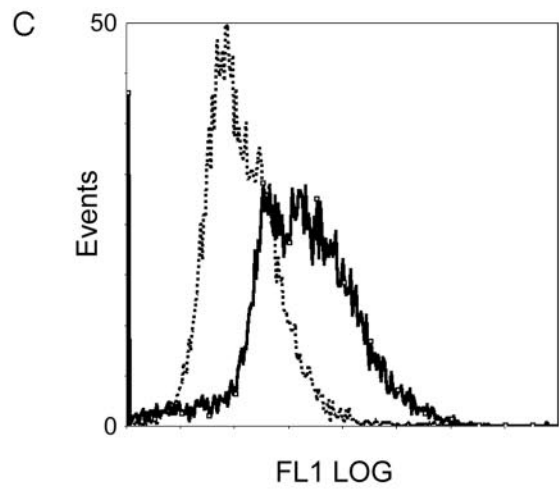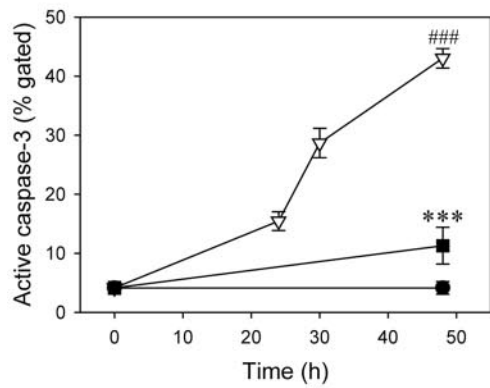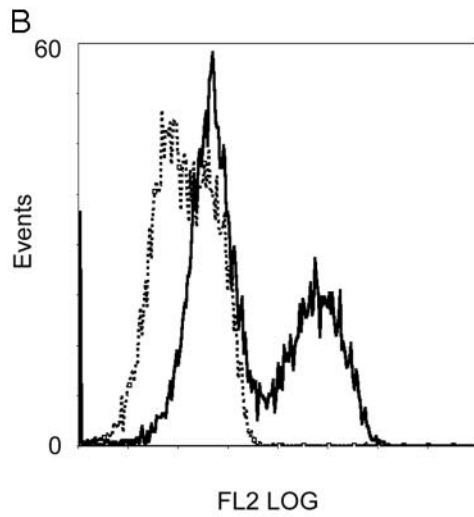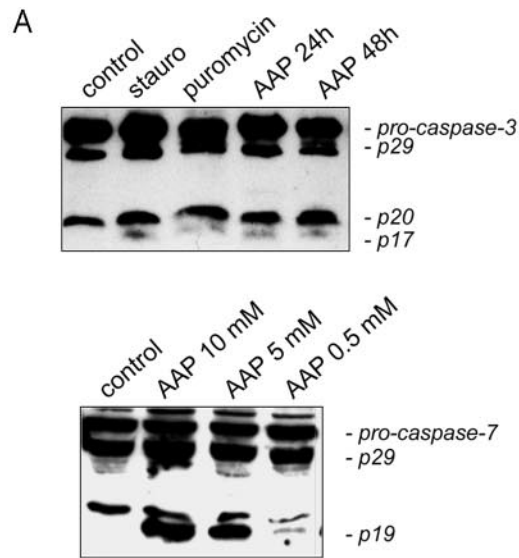
The appearance of the cleaved fragments does not necessarily imply that the caspases were catalytically active. However, the latter was demonstrated by examining the in situ cleavage of the substrate α-fodrin and the formation of a band corresponding to the p120 fragment of α-fodrin. Likewise, the detection of the M30 immunoreactive neoepitope formed as a result of cytokeratin-18 cleavage confirmed the in situ activity of the execution caspases (Fig. 2C). The pivotal role of caspases in AAP-induced HuH7 cell apoptosis was established by the ability of the pan-caspase inhibitor Z-VAD-fmk to block cell death (Fig. 2D) and caspase-mediated proteolysis in situ (Fig. 2C). The cytoprotective effect of the caspase inhibitor was dose-dependent with 50 μM causing a 50% decrease in loss of cell viability and near complete protection was obtained with 100 μM. A significant albeit incomplete protection from AAP-induced cytotoxicity also was obtained with the caspase-specific inhibitor Ac-DEVD-CHO [cytotoxicity (%) at 54 h: AAP, 51.6 ± 10.8; AAP + 200 μM Ac-DEVD-CHO, 39.5 ± 1.9; $p < 0.05$]. However, no protection occurred with the analog Z-FA-fmk (50 μM) that was used as a negative control to rule out possible nonspecific effects of the fmk moiety [cytotoxicity (%) at 54 h: AAP, 53.5 ± 5.6; AAP + 50 μM Z-FA-fmk, 58.4 ± 1.4 ($n = 3$)]. Moreover, N-acetyl-Leu-Leu-Nle-CHO (range 1–10 μM), PD 150606

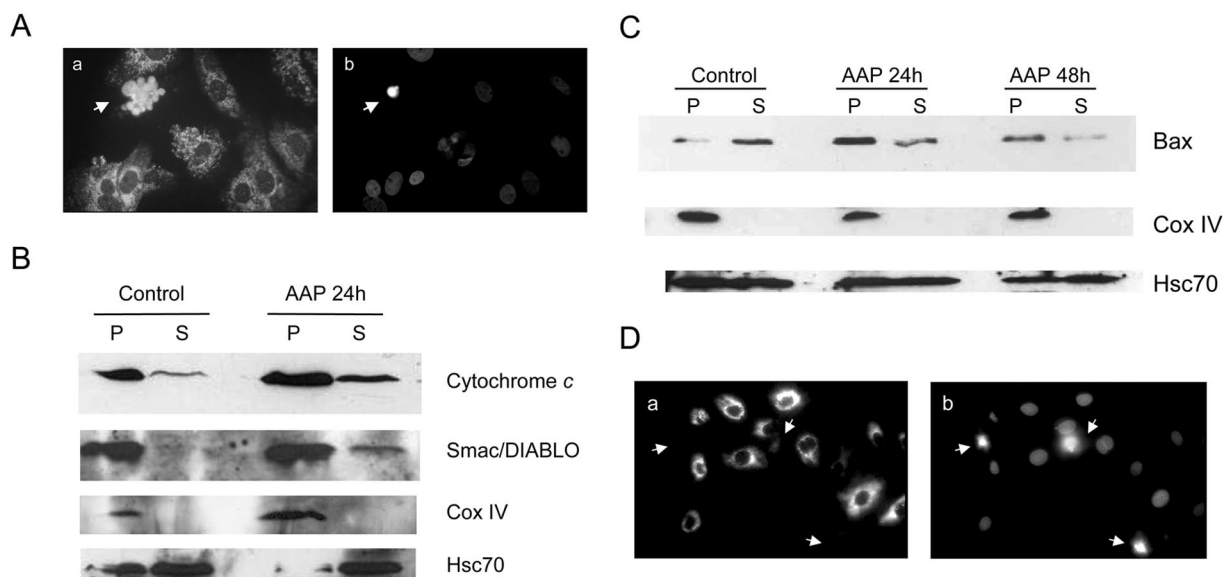(range 1–10 μM), MG-132 (range 0.5–10 μM), or N-tosyl-L-phenylalanine chloromethyl ketone (range 1–10 μM) failed to protect from AAP-induced cytotoxicity (data not shown). These findings demonstrate that cytoprotection was achieved through caspase inhibition rather than interference with cathepsins or calpain activity by the reactive fmk moiety.

Role of Mitochondria in AAP-Induced Apoptosis. AAP-induced apoptosis involved the release of the proapoptotic proteins, including cytochrome c from mitochondria in HuH7 cells (Fig. 3). At the cellular level, the relocation of cytochrome c from mitochondria always correlated with the onset of chromatin condensation (Fig. 3A). Furthermore, the release of mitochondrial intermembrane space proteins was not restricted to cytochrome c and also was observed with Smac/DIABLO (Fig. 3B). The mobilization of the proapoptotic mitochondrial proteins correlated with the translocation of Bax to the mitochondrial membranes (Fig. 3C) as well as a loss of mitochondrial membrane potential ($\Delta\Psi$m) (Fig. 3D). As shown in Fig. 3D, the loss of $\Delta\Psi$m in response to AAP coincided with a corresponding increase in nuclear staining by Hoechst 33258. The onset of apoptosis is characterized by an enhanced fluorescence of the nucleus that precedes the loss of cell viability (Ormerod et al., 1993). Two stages of $\Delta\Psi$m loss as evidenced by TMRE staining were observed (Fig. 3D). In the first stage, near complete loss of TMRE uptake occurred in conjunction with enhanced nuclear staining. However, at this stage no chromatin condensation had taken place. Subsequently, TMRE fluorescence was undetectable but chromatin condensation was observed.

Both the loss of mitochondrial membrane potential and the release of proapoptotic proteins could have resulted from the induction of the mitochondrial permeability transition through pore opening (PTP). Indeed, the induction of PTP in isolated rat liver mitochondria by NAPQI and its dimethylated analogs is well established (Weis et al., 1992). However, in the present study, neither cyclosporin A nor bongkrekic acid was able to prevent or delay the loss of cell viability caused by AAP (Fig. 4).

GSK-3 but Not Stress Kinases Is Involved in AAP-Induced Apoptosis. Given that the interaction between AAP and mitochondria seemed to be indirect and not mediated by NAPQI-induced mitochondrial PTP opening suggests the involvement of an upstream signal(s) that cooperates with Bax to initiate apoptosis. The primary site of AAP metabolism and its bioactivation to NAPQI is the ER. Hence, localized damage within this organelle may play a crucial role in the initiation of a cellular stress response that triggers the mitochondrial pathway of apoptosis. We therefore investigated the role of the MAP kinase pathway members JNK, p38 MAP kinase, and extracellular signal-regulated kinase in AAP-induced apoptosis. Figure 5A shows that two weak bands corresponding to phospho-JNK were detected in control cells. The intensity of the top band was markedly enhanced in AAP-treated cells, which is in contrast to the preferential phosphorylation of the bottom band by the redox-cycling agent duroquinone (500 μM). Together, phosphorylation of JNK occurs in response to AAP treatment, although the pattern is distinct from that elicited by reactive oxygen species. The role of JNK activation in the induction of apoptosis was probed by using the JNK inhibitor SP 600125, and our results show that inhibition of JNK activity did not prevent the loss of cell viability in response to AAP (Fig. 5B).

A

control stauro puromycin AAP 24h AAP 48h

- pro-caspase-3
- p29

- p20
- p17

control AAP 10 mM AAP 5 mM AAP 0.5 mM

- pro-caspase-7
- p29

- p19

B

Events

FL2 LOG

60

Active caspase-3 (% gated)

###

***

Time (h)

C

Events

FL1 LOG

50

Cytokeratin-18 cleavage (% gated)

###

***

Time (h)

control stauro puromycin AAP 10 mM

- Fodrin

- p145

- p120

D

Cell death (%)

#

###

###

###

*

*

*

**

***

***

Time (h)

Fig. 3. Release of apoptogenic factors from mitochondria, Bax translocation and loss of mitochondrial ΔΨm. HuH7 cells were exposed to 10 mM AAP for 24 h before immunostaining for cytochrome c (a, cytochrome c; b, Hoechst 33258-counterstained cells) (A), Western blot analysis of mitochondrial (P) or cytosolic (S) content of cytochrome c and Smac/DIABLO (B), and Western blot analysis of P or S content of Bax were performed as described under *Materials and Methods* (C). Loading controls were done by reprobing the blots for COX IV and Hsc70. D. HuH7 cells grown on glass coverslips were treated with 10 mM AAP for 24 h before staining with 500 nM TMRE and 2 μg/ml Hoechst 33258 and transferring to a Zeiss POC chamber. The cells were viewed on a Zeiss Axiovert 135 fluorescence microscope for TMRE fluorescence (a) and Hoechst 33258 fluorescence (b). Cells undergoing apoptosis are indicated by arrows. Original magnification, 400×.
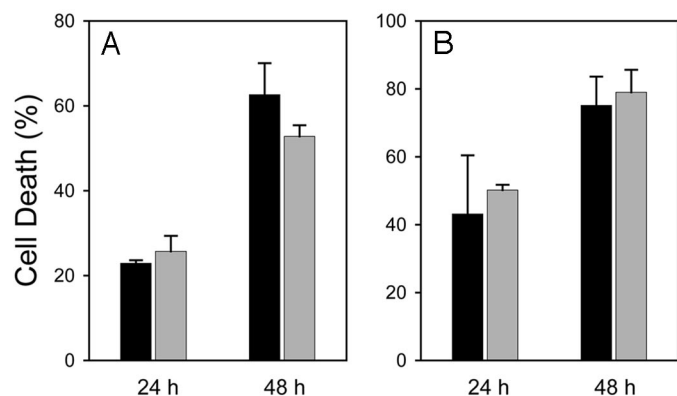

Fig. 4. Inhibitors of the mitochondrial PTP do not protect from acetaminophen-induced cytotoxicity. HuH7 cells were treated with 10 mM AAP in the absence (black shaded) or presence (gray shaded) of 1 μM cyclosporin A (A) or 50 μM bongkrekic acid (B) before assaying for the loss of cell viability as described under *Materials and Methods*. Data are the mean ± S.D. of three independent experiments.

The pharmacological inhibition of p38 MAP kinase activity or MEK1/2 activity by 10 μM SB-203580 and 50 μM PB98059, respectively, also failed to protect or modify AAP cytotoxicity (Fig. 5B). These findings support the conclusion that the members of the MAP kinase pathways studied here are not

involved in AAP-induced apoptosis in HuH7 cells. In contrast, pretreatment with LiCl significantly protected the cells by delaying both the onset and extent of loss of cell viability induced by AAP (Fig. 6A). Because GSK-3 is the primary pharmacological target of LiCl, these data suggest that GSK-3 plays a critical role in the events leading to the cytotoxicity of AAP. This was further confirmed by using two additional and specific inhibitors of this enzyme, SB-216763 and SB-415286 (Coghlan et al., 2000) (Fig. 6B). To rule out the possibility that the inhibitors of GSK-3 were cytoprotective by delaying the onset of secondary necrosis, we tested both SB-415286 and SB-216763 for their ability to prevent caspase-3 activation and hence the execution of apoptosis. Figure 6C demonstrates that the processing of procaspase-3 to its active fragment was significantly inhibited by SB-415286 (48 h: control, 2.8 ± 1.0%; AAP, 29.3 ± 3.5%; AAP + SB-415286, 20.0 ± 2.1%; $p < 0.05$) to a similar extent as the loss of cell viability. Similar results were obtained with SB-216763 (data not shown).

A Role for ER Stress in AAP-Induced Apoptosis? GSK-3 has recently been shown to represent a link between ER stress and the activation of the mitochondrial pathway of apoptosis (Song et al., 2002; Ghribi et al., 2003). We therefore investigated the ability of GSK-3 inhibitors to modulate ER

Fig. 2. Processing of execution procaspases-3 and -7 in acetaminophen-induced apoptosis. A, HuH7 cells were exposed to 10 mM AAP for 24 or 48 h or to 1 μM staurosporine for 24 h or 20 μM puromycin for 24 h, harvested, and probed for the processing of procaspase-3 by Western blot analysis. Similarly, HuH7 cells were treated with 0.5, 5, or 10 mM AAP for 48 h, 1 μM staurosporine for 24 h, or 20 μM puromycin for 24 h and examined for the activation of caspase-7. B, immunodetection of active (processed) caspase-3 by flow cytometry. Top, histogram showing the presence of active caspase-3 in control cells (dotted line) or after exposure to 10 mM AAP for 48 h (straight line). Bottom, time course of procaspase-3 processing after exposure to 10 mM AAP. C, cleavage of cytokeratin-18 and α-fodrin in response to AAP. Control HuH7 cells (dotted line) and cells treated with 10 mM AAP (straight line) were harvested after 48 h, immunostained for cleaved cytokeratin-18, and analyzed by flow cytometry. The time course of cytokeratin-18 cleavage is shown in the middle [control cells, circles; cells treated with AAP in the absence (triangles) or presence (squares) of Z-VAD-fmk (100 μM)]. Bottom, cleavage of α-fodrin in AAP-induced apoptosis. HuH7 cells were treated with 10 mM AAP for 48 h, staurosporine or puromycin (as described above) before immunoblotting for α-fodrin. D, AAP-induced apoptosis requires caspases. HuH7 cells, untreated (closed circles) or treated with 10 mM AAP in the absence (open triangles) or presence of Z-VAD-fmk (50 μM, squares; 150 μM, closed triangles), were assayed for loss of cell viability as measured by the release of cellular lactate dehydrogenase activity. Each point is the mean ± S.D. of three independent experiments. *, $p < 0.05$; **, $p < 0.01$; ***, $p < 0.001$ (AAP + Z-VAD-fmk versus AAP alone); #, $p < 0.05$; ###, $p < 0.001$ (AAP versus control).

A

B
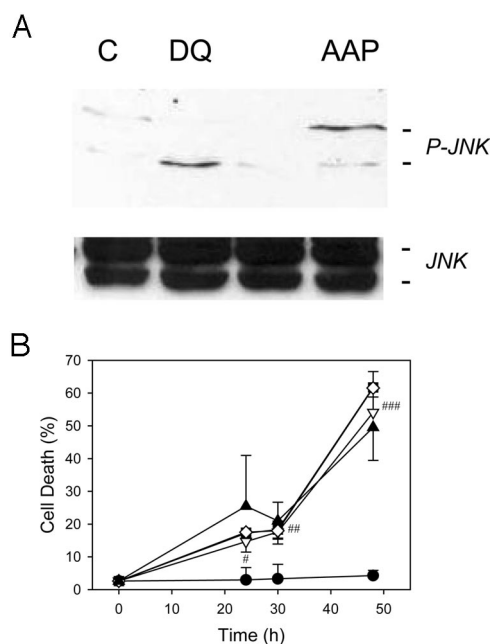
Fig. 5. Acetaminophen induces the phosphorylation of JNK but its toxicity is insensitive to inhibitors of MAP kinase pathways. A, HuH7 cells, controls or treated with 10 mM AAP for 48 h or 500 μM duroquinone (DQ) for 24 h were harvested and probed for phospho-JNK by Western blot analysis. Loading controls were carried out by reprobing the blots for total cellular JNK. B, HuH7 cells, untreated (closed circles) or treated with 10 mM AAP in the absence (open triangles) or presence of 30 μM SP600125 (closed triangles), 10 μM SB-203580 (diamonds), or 50 μM PB98059 (squares) were assayed for loss of cell viability as measured by the release of cellular lactate dehydrogenase activity. Each point is the mean $\pm$ S.D. of three independent experiments. #, $p < 0.05$; ##, $p < 0.01$; ###, $p < 0.001$ (AAP versus control).

stress-induced apoptosis in HuH7 cells. Using the sarco(endo)plasmic reticulum Ca^{2+} ATPase ATPase inhibitor thapsigargin that is well known to induce a condition of ER stress (Kass and Orrenius, 1999), we found that GSK-3 inhibitors blocked thapsigargin-induced apoptosis to a similar degree as their inhibition of AAP-induced apoptosis (Fig. 7A). In contrast, the induction of apoptosis by duroquinone-generated reactive oxygen species was essentially insensitive to GSK-3 inhibition (Fig. 7B).

Discussion

Apoptosis plays a critical role in the mouse in initiating the events that lead to the destruction of the liver after a hepatotoxic dose of AAP (El-Hassan et al., 2003). However, the ability to study the mechanism of AAP-induced apoptosis under in vitro conditions has been hampered by the lack of appropriate in vitro cellular model. Primary cultures of rat hepatocytes respond to cytotoxic doses of AAP by necrosis (Neuman et al., 1999; Nagai et al., 2002) and are therefore an unsuitable model system for the investigation of the early apoptotic events that occur after in vivo administration of AAP. Likewise, the differentiated transgenic mouse hepatocyte cell line (TAMH cells) displays only incomplete biochemical evidence for apoptosis, although some degree of chromatin condensation and caspase activation was reported (Pierce et al., 2002). Inhibition of the latter with z-VAD-fmk failed to prevent AAP-induced TAMH cell death (Pierce et al., 2002). In contrast, AAP-induced apoptosis in HuH7 cells as determined by chromatin condensation and fragmentation, the

A

B

C
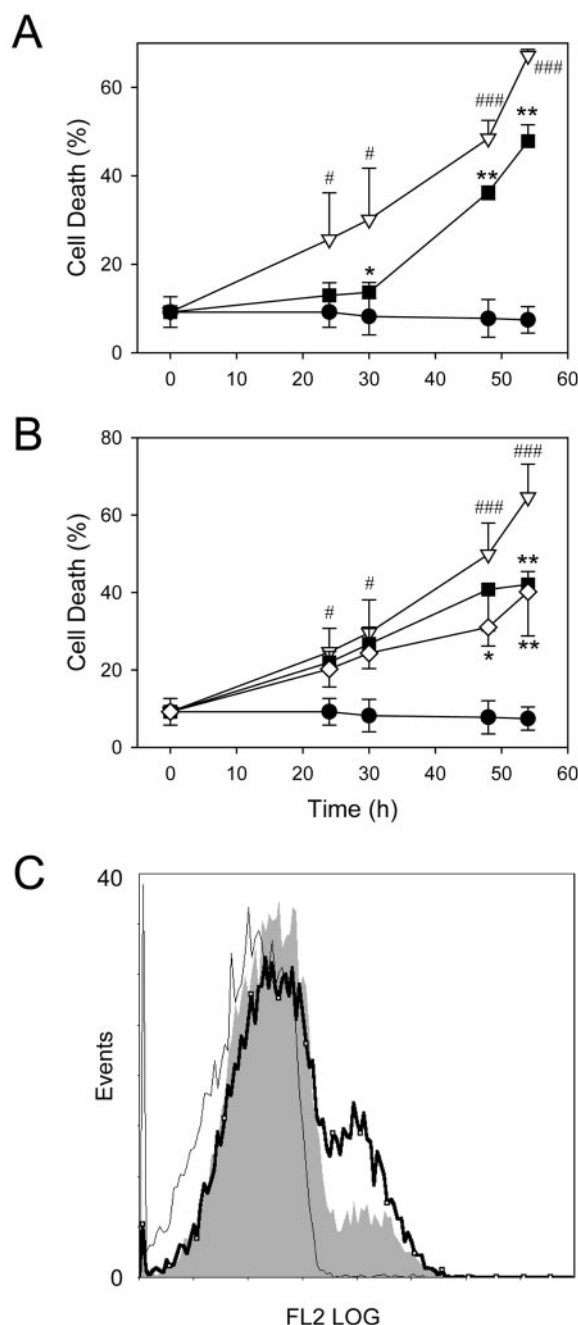
Fig. 6. GSK-3 mediates acetaminophen-induced apoptosis. A, HuH7 cells, untreated (closed circles) or treated with 10 mM AAP in the absence (open triangles) or presence of 20 mM LiCl (squares) were assayed for loss of cell viability as measured by the release of cellular lactate dehydrogenase activity. B, effect of the GSK-3 inhibitors SB-216763 (25 μM, squares) and SB-415286 (3 μM, diamonds) on AAP-induced cell death. C, protection from AAP-induced cell death was caused by a decrease in caspase-3 activation. The histogram shows the presence of active caspase-3 as detected by flow cytometry in control cells (thin line) or after exposure to 10 mM AAP for 48 h in the absence (thick line) or presence (shaded) of 3 μM SB-415286. The cells were preincubated with the GSK-3 inhibitors for 1 h before the addition of AAP. Each point is the mean $\pm$ S.D. of three independent experiments. *, $p < 0.05$; **, $p < 0.01$ (AAP + inhibitor versus AAP alone); #, $p < 0.05$; ###, $p < 0.001$ (AAP versus control).

release of proapoptotic factors from mitochondria, and the activation of caspases. The observations that HuH7 cell death by AAP was critically dependent on caspase activity and that z-VAD-fmk nearly completely blocked AAP-induced
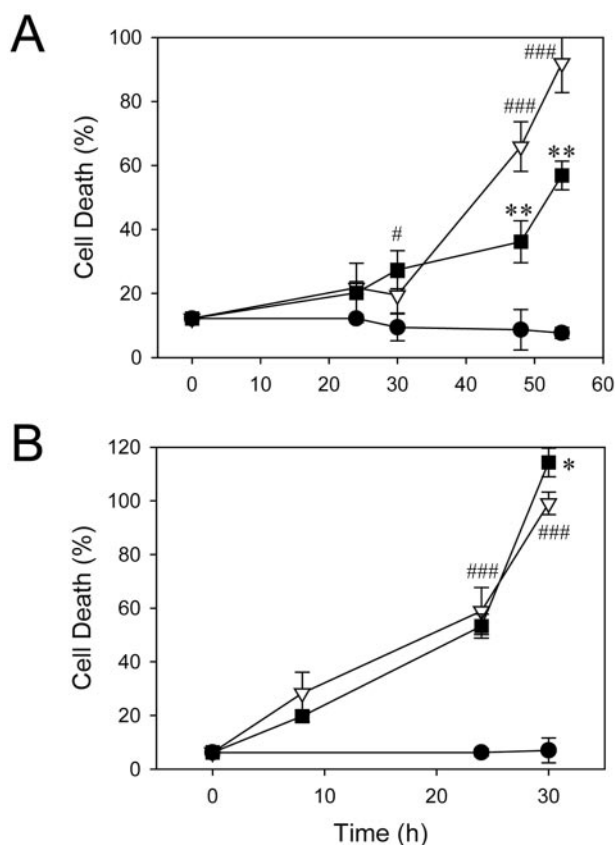
Fig. 7. Role of GSK-3 in ER stress-mediated apoptosis. HuH7 cells were treated with 1 μM thapsigargin (A) or 500 μM duroquinone (B) in the absence (triangles) or presence (squares) of 3 μM SB-415286 (A) or 20 mM LiCl (B). Control cells are represented by the circles. Cytotoxicity was assayed at the indicated time points as described under *Materials and Methods*. Data are the mean ± S.D. of three independent experiments. *, $p < 0.05$; **, $p < 0.01$ (thapsigargin or duroquinone + inhibitor versus thapsigargin or duroquinone alone); #, $p < 0.05$; ###, $p < 0.001$ (thapsigargin or duroquinone versus control).

cell death suggest that apoptosis rather than necrosis was the major form of cell death elicited by AAP. This conclusion is based on reports that caspase inhibitors are unable to block cell death by necrosis (Denecker et al., 2001; Nagai et al., 2002). It should be stressed, however, that the initial apoptotic response elicited in HuH7 cells did not prematurely degenerate into the necrosis typically observed in vivo. The mechanism underlying this transition in cell death mode is unclear. Therefore, HuH7 cells were found to be a good model for the investigation of the mechanism of AAP-induced apoptosis, but the model is not intended to represent the later stages of liver injury. While this work was in progress, a report was published showing that AAP also induced a caspase-mediated apoptotic response in SK-Hep1 cells (Boulares et al., 2002).

AAP induced the release of proapoptotic factors such as cytochrome *c* and Smac/DIABLO into the cytosol. Two mechanisms have been postulated for the activation of this pathway and were investigated here. The release of mitochondrial proapoptotic factors could have been the result of mitochondrial PTP opening. The mitochondrial PTP is believed to be a protein complex formed primarily by outer membrane porin, the adenine nucleotide translocators, and cyclophilin D. Indeed, the pharmacological inhibition of mitochondrial PTP

opening has been demonstrated to prevent apoptosis and cell death in liver cells after exposure to a variety of apoptosis-inducing triggers (Pastorino and Hoek, 2000; Yerushalmi et al., 2001; Zhao et al., 2003). However, neither cyclosporin A nor bongkrekic acid prevented or attenuated AAP-induced HuH7 cell apoptosis. This suggests that the mitochondrial pathway of apoptosis was not initiated by mitochondrial PTP opening.

The execution of AAP-induced apoptosis was dependent on caspases as demonstrated by the protection afforded by caspase inhibitors Z-VAD-fmk and Ac-DEVD-CHO. The pan-caspase inhibitor Z-VAD-fmk was a more potent inhibitor due to its superior ability to penetrate cells and to irreversibly inactivate most cellular caspases compared with the tetrapeptide inhibitor. Nonspecific effects of the reactive fmk moiety leading to the inhibition of cathepsins and calpains were ruled out by the findings that Z-FA-fmk and calpain inhibitors did not affect the cytotoxicity of AAP. Moreover, the cytoprotection provided by Z-VAD-fmk compared well with the prevention of caspase-3 processing and its in situ proteolytic activity. The pharmacological inhibition of calpains or cathepsins did not affect AAP-induced apoptosis, ruling out their role in AAP-induced apoptosis. A recent report (Pierce et al., 2002) showed that inhibition of proteasomal activity in TAMH cells with a low concentration of MG-132 promoted chromatin condensation and nuclear fragmentation induced by AAP, whereas in the absence of the proteasome inhibitor only chromatin margination to the nuclear envelope was observed. Here, no modulation of AAP-induced apoptosis by MG-132 was observed, possibly because a full apoptotic response was already elicited by AAP in HuH7 cells. Together, our results suggest that noncaspase proteases did not independently contribute to the initiation or execution of apoptosis in HuH7 cells by the hepatotoxic drug. However, a striking difference between the response of HuH7 cells to AAP and the in vivo situation is that after administration of AAP in mice, the caspase cascade, although required for the initiation of the events leading to the destruction of the liver, failed to fully activate the downstream execution caspases-3 and -7 (El-Hassan et al., 2003). This leaves open the possibility that noncaspase proteases may contribute to liver cell death downstream of caspases under in vivo conditions and be responsible for some of the necrotic features observed after an hepatotoxic dose of AAP (Adams et al., 2001; Pierce et al., 2002; Jaeschke et al., 2004).

If the trigger for activation of the mitochondrial pathway is not through PTP opening, then an alternative mechanism that most likely participates with Bax needs to be considered. AAP is bioactivated in the ER to the reactive metabolite NAPQI and AAP-induced injury also leads to cellular oxidative stress. Hence, a cellular stress response may be involved in AAP-induced apoptosis. Indeed, recent evidence has shown that AAP activates JNK in a glioma cell line (Bae et al., 2001). Our results demonstrate that JNK is activated before apoptosis, as evidenced by the detection of the corresponding phospho-JNK bands. Interestingly, the pattern of activation was distinct from that elicited by the redox-cycling quinone duroquinone, suggesting that oxidative damage to cells in AAP-induced cytotoxicity (Tirmenstein and Nelson, 1990) is not the primary mechanism of JNK activation in HuH7 cells. However, in contrast to the proapoptotic role of JNK in glioma cell apoptosis, the pharmacological inhibition of JNK activity did not alter AAP-induced apoptosis of HuH7

cells. Likewise, the inhibition of p38 MAP kinase or MEK1/2 failed to modulate the ability of AAP to trigger apoptosis in the hepatoma cells. Although a cellular specificity intrinsic to HuH7 cells cannot be excluded, these findings lead to the conclusion that neither the stress kinase pathways nor the extracellular signal-regulated kinase pathway of the MAP kinase family of signaling pathways is involved in AAP-induced liver cell apoptosis. This is in contrast to inducers of liver cell apoptosis such as menadione and tumor necrosis factor whose mechanisms of apoptosis action have been causally linked to the activation of one or more MAP kinase pathways (Czaja et al., 2003; Pastorino et al., 2003).

GSK-3β is now recognized as being a central regulator of apoptosis and cell survival (Jope and Johnson, 2004). In cells, this enzyme is maintained in an inactive state among others by AKT-, p90^{RSK}-, and protein kinase A-mediated phosphorylation of N-terminal serine-9 and other mechanisms (Jope and Johnson, 2004). Activation of GSK-3 results in the up-regulation of a number of proapoptotic genes and down-regulation of antiapoptotic genes through its effect on a wide number of transcription factors. Hence, its silencing is important in survival signals against a wide range of apoptosis-inducing conditions. Much of our current knowledge on the role of GSK-3β in apoptosis stems from work in the area of neurodegeneration, and relatively little is known about its potential role in liver cells. Yet, GSK-3β deficiency in mice is embryolethal as a result of massive liver degeneration in mid-gestation. This is caused by a failure of protection from tumor necrosis factor-induced apoptosis by GSK-3 mediated p65 phosphorylation and nuclear factor-κB transactivation (Schwabe and Brenner, 2002). We therefore investigated the potential role of GSK-3 in AAP-induced apoptosis, and as reported here, a proapoptotic function was uncovered. A comparison with other inducers of apoptosis in HuH7 cells showed that the apoptotic effect of reactive oxygen species was insensitive to GSK-3 inhibition but that thapsigargin-mediated apoptosis was decreased by a similar degree as AAP-induced apoptosis in the presence of LiCl, SB-216763, or SB-415286. These findings show that GSK-3 plays a fundamental role in ER stress-induced apoptosis in HuH7 liver cells that is similar to its role in neuronal cells (Song et al., 2002; Ghribi et al., 2003). Moreover, our data support the hypothesis that AAP triggers an ER stress response in these cells. This response is most likely to occur during the bioactivation of AAP to NAPQI, which takes place in the ER by cytochrome P450-mediated metabolism (Tonge et al., 1998; Zaher et al., 1998). Indeed, it was recently suggested that AAP-mediated renal tubular injury involved ER stress (Lorz et al., 2004). Together, our findings suggest that AAP induces an ER stress response and that GSK-3 provides a mechanistic link between the ER and the ensuing activation of the mitochondrial pathway of apoptosis. However, the molecular mechanisms involved remain to be elucidated.

In conclusion, AAP induces apoptosis in HuH7 liver cells by activating the mitochondrial pathway of apoptosis through the release of proapoptotic factors such as cytochrome c and Smac/DIABLO and downstream caspase activation. GSK-3 was identified as a major regulator of the apoptotic response and is proposed to functionally link AAP-induced ER stress to the mitochondrial pathway of apoptosis.

References

Adams ML, Pierce RH, Vail ME, White CC, Tonge RP, Kavanagh TJ, Fausto N, Nelson SD, and Bruschi SA (2001) Enhanced acetaminophen hepatotoxicity in transgenic mice overexpressing BCL-2. *Mol Pharmacol* **60:**907–915.

Bae MA, Pie JE, and Song BJ (2001) Acetaminophen induces apoptosis of C6 glioma cells by activating the c-Jun NH$_2$-terminal protein kinase-related cell death pathway. *Mol Pharmacol* **60:**847–856.

Blazka ME, Elwell MR, Holladay SD, Wilson RE, and Luster MI (1996) Histopathology of acetaminophen-induced liver changes: role of interleukin-1α and tumor necrosis factor α. *Toxicol Pathol* **24:**181–189.

Boulares AH, Zoltoski AJ, Stoica BA, Cuvillier O, and Smulson ME (2002) Acetaminophen induces a caspase-dependent and Bcl-x(L) sensitive apoptosis in human hepatoma cells and lymphocytes. *Pharmacol Toxicol* **90:**38–50.

Coghlan MP, Culbert AA, Cross DAE, Corcoran SL, Yates JW, Pearce NJ, Rausch OL, Murphy GJ, Carter PS, Cox LR, et al. (2000) Selective small molecule inhibitors of glycogen synthase kinase-3 modulate glycogen metabolism and gene transcription. *Chem Biol* **7:**793–803.

Cohen SD, Pumford NR, Khairallah EA, Boekelheide K, Pohl LR, Amouzadeh HR, and Hinson JA (1997) Selective protein covalent binding and target organ toxicity. *Toxicol Appl Pharmacol* **143:**1–12.

Czaja MJ, Liu HL, and Wang YJ (2003) Oxidant-induced hepatocyte injury from menadione is regulated by ERK and AP-1 signaling. *Hepatology* **37:**1405–1413.

Dargan PI and Jones AL (2003) Management of paracetamol poisoning. *Trends Pharmacol Sci* **24:**154–157.

Denecker G, Vercammen D, Steemans M, Vanden Berghe T, Brouckaert G, Van Loo G, Zhivotovsky B, Fiers W, Grooten J, Declercq W, et al. (2001) Death receptor-induced apoptotic and necrotic cell death: differential role of caspases and mitochondria. *Cell Death Differ* **8:**829–840.

Dixon MF, Dixon B, Aparicio SR, and Loney DP (1975) Experimental paracetamol-induced hepatic necrosis: a light- and electron-microscope and histochemical study. *J Pathol* **116:**17–29.

El-Hassan H, Anwar K, Macanas-Pirard P, Crabtree M, Chow SC, Johnson VL, Lee PC, Hinton RH, Price SC, and Kass GEN (2003) Involvement of mitochondria in acetaminophen-induced apoptosis and hepatic injury: roles of cytochrome c, Bax, Bid and caspases. *Toxicol Appl Pharmacol* **191:**118–129.

Ferret P-J, Hammoud R, Tulliez M, Tran A, Trébéden H, Jaffray P, Malassagne B, Calmus Y, Weill B, and Batteux F (2001) Detoxification of reactive oxygen species by a nonpeptidyl mimic of superoxide dismutase cures acetaminophen-induced acute liver failure. *Hepatology* **33:**1173–1180.

Ghribi O, Herman MM, and Savory J (2003) Lithium inhibits Abeta-induced stress in endoplasmic reticulum of rabbit hippocampus but does not prevent oxidative damage and tau phosphorylation. *J Neurosci Res* **71:**853–862.

Gujral JS, Knight TR, Farhood A, Bajt ML, and Jaeschke H (2002) Mode of cell death after acetaminophen overdose in mice: apoptosis or oncotic necrosis? *Toxicol Sci* **67:**322–328.

Jaeschke H, Gujral JS, and Bajt ML (2004) Apoptosis and necrosis in liver disease. *Liver Int* **24:**85–89.

Jones RA, Johnson VL, Buck NR, Dobrota M, Hinton RH, Chow SC, and Kass GEN (1998) Fas-mediated apoptosis in mouse hepatocytes involves the processing and activation of caspases. *Hepatology* **27:**1632–1642.

Jope RS and Johnson GVW (2004) The glamour and gloom of glycogen synthase kinase-3. *Trends Biochem Sci* **29:**95–102.

Kass GEN and Orrenius S (1999) Calcium signaling and cytotoxicity. *Environ Health Perspect* **107 (Suppl 1):**25–35.

Kaufmann SH (2001) Reutilization of immunoblots after chemiluminescent detection. *Anal Biochem* **296:**283–286.

Knight TR and Jaeschke H (2002) Acetaminophen-induced inhibition of Fas receptor-mediated liver cell apoptosis: mitochondrial dysfunction versus glutathione depletion. *Toxicol Appl Pharmacol* **181:**133–141.

Li S, Zhao Y, He X, Kim TH, Kuharsky DK, Rabinovitch H, Chen J, Du C, and Yin XM (2002) Relief of extrinsic pathway inhibition by the Bid-dependent mitochondrial release of Smac in Fas-mediated hepatocyte apoptosis. *J Biol Chem* **277:**26912–26920.

Lorz C, Justo P, Sanz A, Subira D, Egido J, and Ortiz A (2004) Paracetamol-induced renal tubular injury: a role for ER stress. *J Am Soc Nephrol* **15:**380–389.

Nagai H, Matsumaru K, Feng GP, and Kaplowitz N (2002) Reduced glutathione depletion causes necrosis and sensitization to tumor necrosis factor-α-induced apoptosis in cultured mouse hepatocytes. *Hepatology* **36:**55–64.

Neuman MG, Cameron RG, Haber JA, Katz GG, Malkiewicz IM, and Shear NH (1999) Inducers of cytochrome P450 2E1 enhance methotrexate-induced hepatocytotoxicity. *Clin Biochem* **32:**519–536.

Ormerod MG, Sun XM, Snowden RT, Davies R, Fearnhead H, and Cohen GM (1993) Increased membrane-permeability of apoptotic thymocytes—a flow cytometric study. *Cytometry* **14:**595–602.

Pastorino JG and Hoek JB (2000) Ethanol potentiates tumor necrosis factor-α cytotoxicity in hepatoma cells and primary rat hepatocytes by promoting induction of the mitochondrial permeability transition. *Hepatology* **31:**1141–1152.

Pastorino JG, Shulga N, and Hoek JB (2003) TNF-alpha-induced cell death in ethanol-exposed cells depends on p38 MAPK signaling but is independent of bid and caspase-8. *Am J Physiol* **285:**G503–G516.

Pierce RH, Franklin CC, Campbell JS, Tonge RP, Chen WC, Fausto N, Nelson SD, and Bruschi SA (2002) Cell culture model for acetaminophen-induced hepatocyte death in vivo. *Biochem Pharmacol* **64:**413–424.

Prescott LF (1996) *Paracetamol (Acetaminophen): A Critical Bibliographic Review*, Taylor & Francis Ltd., London.

Qiu YC, Benet LZ, and Burlingame AL (1998) Identification of the hepatic protein targets of reactive metabolites of acetaminophen in vivo in mice using two-dimensional gel electrophoresis and mass spectrometry. *J Biol Chem* **273:**17940–17953.

Ray SD, Sorge CL, Raucy JL, and Corcoran GB (1990) Early loss of large genomic DNA in vivo with accumulation of Ca^{2+} in the nucleus during acetaminophen-induced liver injury. *Toxicol Appl Pharmacol* **106:**346–351.

Salgia ADT and Kosnik SD (1999) When acetaminophen use becomes toxic—treating acute accidental and intentional overdose. *Postgrad Med* **105:**81–84.

Schwabe RF and Brenner DA (2002) Role of glycogen synthase kinase-3 in TNF-alpha-induced NF-kappa B activation and apoptosis in hepatocytes. *Am J Physiol* **283:**G204–G211.

Song L, De Sarno P, and Jope RS (2002) Central role of glycogen synthase kinase-3 beta in endoplasmic reticulum stress-induced caspase-3 activation. *J Biol Chem* **277:**44701–44708.

Tirmenstein MA and Nelson SD (1990) Acetaminophen-induced oxidation of protein thiols: contribution of impaired thiol-metabolizing enzymes and the breakdown of adenine nucleotides. *J Biol Chem* **265:**3059–3065.

Tonge RP, Kelly EJ, Bruschi SA, Kalhorn T, Eaton DL, Nebert DW, and Nelson SD (1998) Role of CYP1A2 in the hepatotoxicity of acetaminophen: investigations using *Cyp1a2* null mice. *Toxicol Appl Pharmacol* **153:**102–108.

Weis M, Kass GEN, Orrenius S, and Moldéus P (1992) *N*-Acetyl-*p*-benzoquinone imine induces Ca^{2+} release from mitochondria by stimulating pyridine nucleotide hydrolysis. *J Biol Chem* **267:**804–809.

Yerushalmi B, Dahl R, Devereaux MW, Gumpricht E, and Sokol RJ (2001) Bile acid-induced rat hepatocyte apoptosis is inhibited by antioxidants and blockers of the mitochondrial permeability transition. *Hepatology* **33:**616–626.

Zaher H, Buters JTM, Ward JM, Bruno MK, Lucas AM, Stern ST, Cohen SD, and Gonzalez FJ (1998) Protection against acetaminophen toxicity in CYP1A2 and CYP2E1 double-null mice. *Toxicol Appl Pharmacol* **152:**193–199.

Zhao YG, Ding WX, Qian T, Watkins S, Lemasters JJ, and Yin XM (2003) Bid activates multiple mitochondrial apoptotic mechanisms in primary hepatocytes after death receptor engagement. *Gastroenterology* **125:**854–867.

Address correspondence to: Dr. George E. N. Kass, School of Biomedical and Molecular Sciences, University of Surrey, Guildford, Surrey GU2 7XH, UK. E-mail: g.kass@surrey.ac.uk